CHEMICAL ENGINEERING TRANSACTIONS
VOL. 74, 2019
A publication of AIDIC
The Italian Association of Chemical Engineering
Online at www.cetjournal.it
Guest Editors: Sauro Pierucci, Jiří Jaromír Klemeš, Laura Piazza

ISBN 978-88-95608-71-6; **ISSN** 2283-9216
DOI: 10.3303/CET1974175

Numerical Simulation of New Uniform Circular Obstacles Cross-Flow Micromixers

João L. Silva Jr., J.L.[a], Harrson S. Santana[b,*], Osvaldir P. Taranto[b]

[a] Federal Institute of Education, Science and Technology of South of Minas Gerais, 37560-260, Pouso Alegre, MG, Brazil
[b] School of Chemical Engineering, University of Campinas, 13083-852, Campinas, SP, Brazil
harrison.santana@gmail.com

A new micromixer design based on uniform circular obstacles and cross flow (UCCFM) of the fluid streams was proposed. Water-ethanol and oil-ethanol mixing was assessed for Reynolds numbers ranging from 0.1 to 100 by CFD simulations. The performance index was evaluated providing the ratio of fluid mixing degree (MI) to the unit of pressure drop along the micromixer. For both systems, the highest performance indexes were noticed at Re = 0.01, a flow regime characterized by molecular diffusion controlling the mass transfer. The UCCFM design with diameter = 600 μm allowed good fluid mixing for water-ethanol at Re = 0.01 (MI = 0.815) with a very low pressure drop of 0.123 Pa. For oil-ethanol mixing, the MI = 0.693 was obtained with a pressure drop of 76.06 Pa. The UCCFM presented a superior MI in low Reynolds number regarding other micromixer designs in literature.

1. Introduction

Recently, Microfluidics, defined as the science and technology area handling fluid flow in micrometric channels, has receiving great attention. The potential application of microstructured devices includes chemical and pharmaceutical synthesis, biological analysis, nanoencapsulation (Cerbelli et al., 2017), microsensors, micro heat-exchangers (Silva et al., 2017) and microchannel reactors (Santana et al., 2015; Castell et al., 2009; Whitesides, 2006). The characteristic length scale results in high surface area-to-volume ratio, providing enhanced heat and mass transfer rates. Other advantages of microdevices are easiness of temperature control, subproducts minimization, low amount of reagents and samples, short residence times required and greater safety in the processing of flammable and toxic substances (Pohar e Plazl, 2009; Whitesides, 2006). Another benefit of microdevices is the possibility of a simple integration to other operation units. The main disadvantage is the relative low flow rate, however, several efforts have been performed in scale-up and numbering-up (multiplication of an optimized microdevice for continuous parallel operation) (Zhou et al. 2017; Pistoresi et al., 2015) to overcome this issue. These advantages stand out the great potential of Microfluidics for chemical process intensification. The Computational Fluid Dynamics (CFD) can also be employed as a process intensification tool. The CFD allows design and evaluation of different geometries with a relative low cost and reduced time, since the design performance evaluation can be carried out before manufacturing of the physical prototype and the prediction of flow field in severe operating conditions, where physical experimentation would be very difficult or even impracticable. However, since CFD is a numerical technique, inherent errors of numerical approximations and mathematical model assumptions should always take into account in the results evaluation. Currently, the development and optimization of micromixers has receiving great attention in order to scale-up the devices from micro to milli scale without missing the advantageous transport phenomena characteristics of microscale, however, allowing the operation under higher flow rates. Micromixers consist in channel zones with static obstacles, promoting a passive fluid mixing, usually inducing split and recombination of streams and chaotic advection (local turbulence by vortex generation), using the own fluid flow energy in the mixing process. An efficient or optimal micromixer must promote high fluid mixing with a minimum pressure drop. In this context, micromixers with cross flow were proposed and their performance were assessed for two distinct flow systems: water-ethanol and vegetable oil-ethanol, for the

Paper Received: 19 April 2018; Revised: 28 September 2018; Accepted: 10 February 2019

Please cite this article as: Silva Jr. J., Santana H., Taranto O., 2019, Numerical Simulations of New Uniform Circular Obstacles Cross-flow Micromixers, Chemical Engineering Transactions, 74, 1045-1050 DOI:10.3303/CET1974175

range of Reynolds number from 0.01 to 100. CFD simulations were accomplished and the performance index, the ratio of mixing degree to the microdevice unit pressure drop was evaluated.

2. Methodology

2.1 Case Description and Mathematical Modeling

The mixing performance was accomplished using Computational Fluid Dynamics. The Ansys CFX 17.2 code was used. Binary mixtures were considered for both systems: 1 – water/ethanol; 2 - vegetable oil/ethanol. The first one presents relative low viscosity and good miscibility. For this system, both feeds were considered entering the micromixer with same velocity. In contrast, oil phase is highly viscous, presenting low miscibility with ethyl alcohol. Often, vegetable oil and ethanol are employed in alkaline-media biodiesel synthesis using microreactors as demonstrated by Santana et al. (2017, 2016). For such system, the alcohol/oil molar ratio of 9 was considered in the inlet boundary condition, based on the superior biodiesel yield obtained by Santana et al. (2017). The following assumptions were made in mathematical modeling: incompressible laminar flow, steady-state, isothermal conditions at 50 ºC and no chemical reaction occurrence (only mixing of fluids). Accordingly, the CFD model consisted in the multicomponent approach, solving a single set of continuity (Eq. 1) and Navier-Stokes (Eq. 2) equations. In addition, individual chemical species mass balances are solved (Eq. 3) jointly with a mass fraction restriction (Eq. 4):

$$\nabla \cdot U = 0 \tag{1}$$

$$\rho\left(U \cdot \nabla U\right) = -\nabla\, p + \mu \nabla^2 U + \rho\, g \tag{2}$$

$$\rho\left(U \cdot \nabla Y_A\right) = \rho\, D_{AB}\, \nabla^2 Y_A \tag{3}$$

$$Y_B = 1 - Y_A \tag{4}$$

where U is the velocity, in m s^{-1}, ρ is the specific mass, in kg m^{-3}, p is the pressure, in Pa, μ is the dynamic viscosity, in Pa s^{-1}, g is the gravity acceleration, in m s^{-2}, Y is the chemical species mass fraction, D_{AB} is the mass diffusivity coefficient for the binary mixture, in m^2 s^{-1}, estimated from Wilke-Chang correlation. The mixture transport properties ρ and μ were weighted by the local species mass fraction.

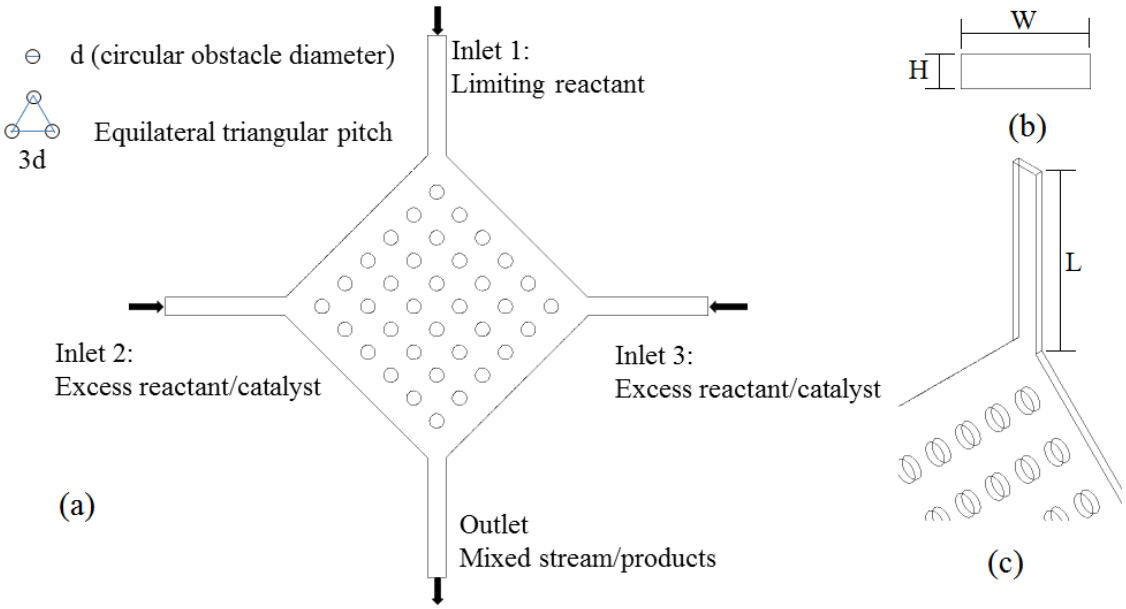

Figure 1 – (a) UCCFM design; (b) inlet/outlet channels cross section; (c) detail of the inlet/outlet length – d: circular obstacle diameter; H = height; W = width; L = length.

The proposed micromixer designs were based in cross flow between the fluids, being designated as Uniform Circular Cross Flow Micromixers (UCCFM) (details are given in Figure 1). The design was conceived to achieve a fast mixing between reagents and homogeneous catalyst. Microchannel reactors could be coupled at the UCCFM outlet channel to complete the chemical reaction. All proposed designs present inlet and outlet channels dimensions of: H = 200 μm (height) x W = 750 μm (width) x L = 5000 μm (length). Circular obstacles were arranged in equilateral triangular pitch of 3d, where d is the circular obstacle diameter. Three obstacle diameters were used: Geometry 1: d = 150 μm; Geometry 2: d = 450 μm; Geometry 3: d = 600 μm.
The transport properties of sunflower (vegetable) oil were taken from Santana et al. (2017). The transport properties for water and ethanol were taken from the material properties library of Ansys CFX. The boundary conditions used are detailed in Table 1 and Figure 1. High order schemes were used in numerical solution and a residual target of 10^{-5} (RMS) was defined for steady-state solving procedure by 500 to 5000 iterations

Table 1: Boundary conditions used in CFD simulations.

Boundary	Condition
Inlet 1	Prescribed velocity according to the Reynolds number Pure water or pure vegetable oil
Inlets 2 and 3	Prescribed velocity according to the Reynolds number Pure ethanol
Outlet	Relative pressure zero (domain reference pressure of 1 atm)
Wall	No-slip

2.2 Spatial Discretization Independence Mesh Test

Firstly, the solution dependence on the spatial discretization was evaluated. Five grid refinement levels were generated and tested for geometry 2 (d = 450 μm), resulting in tridimensional meshes with about 760,000; 1,600,000; 2,460,000; 3,500,000 and 4,300,000 control volumes. The mesh independence was investigated using the micromixer pressure drop and the velocity profile at the outlet channel for the Reynolds number of 100 (advection predominant laminar flow).
Usually, design and optimization studies of devices require simulation and performance analyses of several different geometries, becoming the numerical independence mesh test impracticable for all proposed designs and operating conditions. In this context, the present study performed the numerical independence mesh test based on the geometry with intermediate dimensions, extending the use of independent-grid parameters for the other designs. The average size of the independent grid, h_{grid}, was estimated as proposed by Celik et al. (2008) (Eq. 5). Therefore, all other numerical meshes were generated using h_{grid}, in order to standardize the average element size on all geometries.

$$h_{grid} = \left[\frac{1}{N_{grid}} \sum_{i=1}^{N_{grid}} \left(\Delta V_i \right) \right]^{1/3} \tag{5}$$

where N_{grid} is the total number of tridimensional elements and the summation of individual element volumes, ΔV_i, provides the total fluid domain volume.

2.3 Mixing Performance Evaluation

The design performance was evaluated using the concept of Performance Index, PI, (Eq. 6, in % Pa^{-1}), given as the ratio of the Mixing Index, MI, (Eq. 7) to the pressure drop ($\Delta P = P_{in} - P_{out}$):

$$\mathrm{PI} = \frac{\left(\mathrm{MI} \times 100 \right)}{P_{in} - P_{out}} \tag{6}$$

$$\mathrm{MI} = 1 - \sqrt{\frac{\sigma^2}{\sigma_{\max}^2}} \quad \text{with} \quad \sigma = \sqrt{\frac{\sum \left(Y_n - Y_{ave} \right)^2}{N}} \tag{7}$$

where *MI* quantifies the mixing degree of a chemical species in a cross section, σ is the standard deviation of mass fraction, Y_n is the local mass fraction, Y_{ave} is the average mass fraction in cross section, N is the number of samples, σ_{max} is the maximum deviation of mass fraction, P_{in} is the inlet pressure and P_{out} is the outlet

pressure. The mixing index ranges from 0 (total segregation of fluids) to 1 (perfect fluid mixing). The optimal design performance is given by higher values of performance index, i.e. high mixing indexes with lower pressure drops. The mixing performance was carried out ranging the Reynolds of the non-alcoholic fluid (water and oil) from 0.01 to 100.

3. Results and Discussion

3.1 Independence Mesh Test Results

This step was accomplished by the analysis of pressure drop and axial velocity profile for both systems. Table 2 summarizes the pressure drop deviation based on the prediction provided by the most refined grid. Figure 2 presents the axial velocity profile in the outlet channel for water-ethanol flow (Figure 2a) and oil-ethanol flow (Figure 2b), for an operating condition of Re = 100.

Table 2: Relative deviations (from most refined mesh - 4,300,000*) of pressure drop (%) predicted by different grid refinement levels.*

Flow System	Numerical grid (number of control volumes)			
	760,000	1,600,000	2,460,000	3,500,000
Water-Ethanol	14.99	5.53	6.66	3.43
Oil-Ethanol	15.69	5.86	8.13	3.37

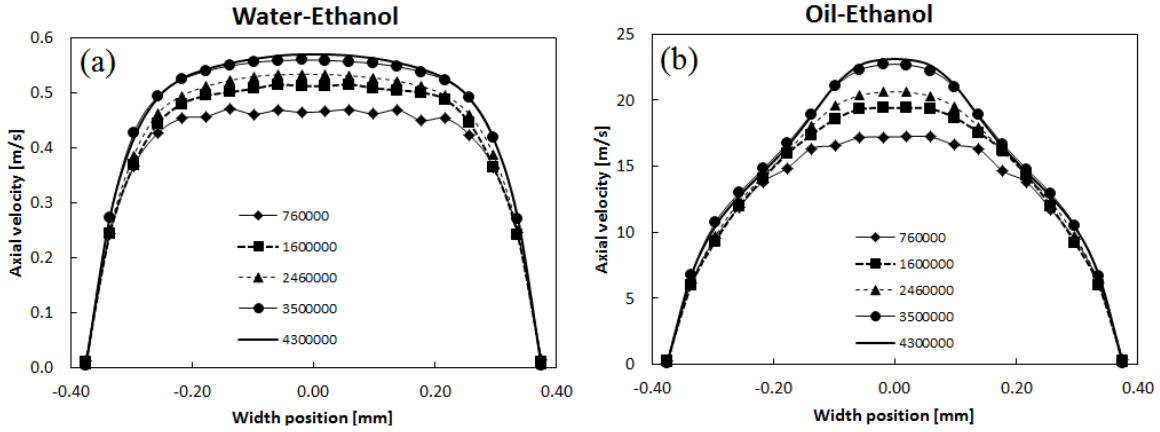

Figure 2 – Axial velocity profiles at outlet channel predicted by different grid refinement levels for: (a) water-ethanol flow; (b) oil-ethanol flow.

The numerical solution independence on spatial discretization was noticed from 3,500,000 elements. From Table 2 was noticed that this refinement level provided the closest pressure drop concerning the most refined grid (reference mesh) for both systems, resulting in deviations of pressure drop below 3.5%. Moreover, analyzing the axial velocity profiles for both systems (Figure 2), the grid composed by 3.5 million elements also presented the closest approximation to the most refined mesh. The coarser meshes resulted in higher deviations, not achieving spatial discretization independence. Despite the higher differences in the velocity profile of both systems, once the flow rate required for oil-ethanol was higher for same Reynolds number, the grid composed by 3,500,000 control volumes provided spatial discretization independence for both flow systems. Based on these results, the 3.5 x 10^6 elements mesh was chosen for further analyses. The h_{grid} from this mesh was 18.16 µm, resulting in grids composed by about N_{grid} = 3.6 x 10^6 (geometry 1, d = 150 µm) and 3.34 x 10^6 (geometry 3, d = 600 µm).

3.2 Fluid Mixing Analysis

The fluids mixing performance was evaluated by ranging the water-based Reynolds number from 0.01 to 100. Figure 3(a,b) presents the predicted Mixing Index (MI) at the outlet channel for the water-ethanol flow. Figure 3(c,d) presents the results for oil-ethanol flow. The PI results are summarized in Table 3.

Table 3: Performance indexes, PI in % Pa^{-1}, obtained for both flow systems in all UCCFM designs.

Flow system	Water-Ethanol			Oil-Ethanol		
Re	d = 150 µm	d = 450 µm	d = 600 µm	d = 150 µm	d = 450 µm	d = 600 µm
0.01	613.63	641.12	661.69	9.11×10^{-1}	9.22×10^{-1}	9.10×10^{-1}
0.1	57.17	58.04	56.28	9.27×10^{-2}	9.45×10^{-2}	9.24×10^{-2}
1	5.44	5.61	5.45	8.78×10^{-3}	8.91×10^{-3}	8.76×10^{-3}
10	0.51	0.53	0.51	8.61×10^{-4}	8.75×10^{-4}	8.59×10^{-4}
50	0.09	0.09	0.09	1.64×10^{-4}	1.68×10^{-4}	1.64×10^{-4}
100	0.04	0.04	0.04	7.67×10^{-5}	7.91×10^{-5}	7.74×10^{-5}

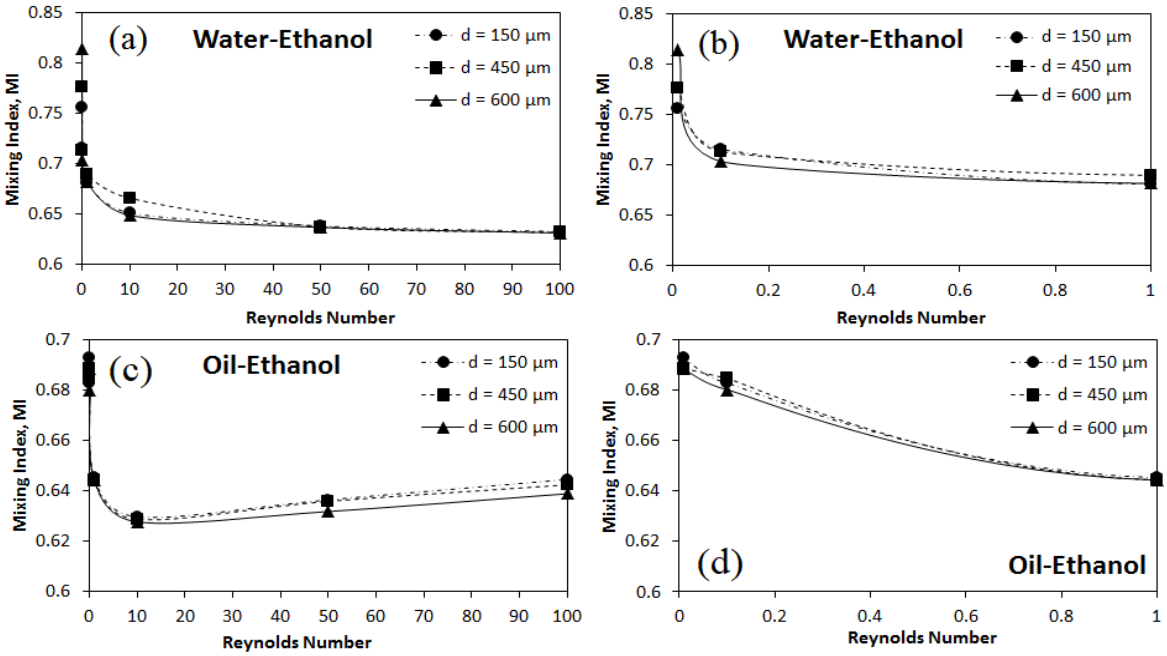

Figure 3 – Mixing Index (MI) obtained for: (a) water-ethanol (Re: 0.01 to 100); (b) water-ethanol (lower Re: 0.01 to 1); (c) oil-ethanol (Re: 0.01 to 100); (d) oil-ethanol (lower Re: 0.01 to 1).

For oil-ethanol system, the mixing index dependence on Reynolds number decrease until the minimum at Re = 10. All three geometries promoted similar results, with slight differences. The higher mixing indexes were 0.693 (PI = 9.11×10^{-3} % Pa^{-1}), 0.689 (PI = 9.22×10^{-3} % Pa^{-1}) and 0.688 (PI = 9.10×10^{-3} % Pa^{-1}) for the obstacle diameters of 150 µm, 450 µm and 600 µm, respectively (Figure 3c,d). Increasing the Reynolds number from 10 to 100, MI slightly increased from about 0.63 to 0.64, however, the PI decrease from about 8.6×10^{-4} % Pa^{-1} to 7.7×10^{-3} % Pa^{-1} (average PI from the geometries) due to the pressure drop increment. The minimum pressure drop of 74.5 Pa was noticed for the geometry 2 (d = 450 µm). The increment of Reynolds number provided shorter residence time for the fluids, not increasing the fluid mixing. In general, the PI decreased with the Reynolds number. Above Re = 10, the three designs presented similar performance. The superior performance index was provided by the geometry 3 (d = 600 µm) for water-ethanol flow. For the viscous oil-ethanol flow, the PI is very low compared to water-ethanol flow, since the pressure drop increased about 600 times. The UCCFM design with d = 600 µm allowed a good fluid mixing for the water-ethanol at Re = 0.01 with a very low pressure drop of 0.123 Pa.

The UCCFM presented a superior MI in low Reynolds number regarding other micromixer designs in literature. As example, the MSE micromixer provided higher mixing index, mostly at elevated Reynolds numbers for the same fluid flow systems (oil-ethanol, Santana et al., 2017), achieving MI = 0.41 at Re = 0.1. For Re = 0.01, the UCCFM provided MI = 0.683, 0.685 and 0.680 for obstacle diameters of 150 µm, 450 µm and 600 µm, respectively. Another advantage of UCCFM is the total size of the micromixer for its manufacturing. The MSE micromixer was manufactured using the soft lithography technique, requiring a total

area of about 2500 mm². Using the same technique, the UCCFM microdevice requires only about 511 mm², reinforcing the efficiency of these new micromixers. Comparing the PI of UCCFM with the obtained by Santana et al. (2017) for the MSE design, the UCCFM presented a performance index (PI_{UCCFM} = 9.45 x 10^{-2}) 12 times superior than MSE (PI_{MSE} = 7.74 x 10^{-3}), showing again the efficiency of the proposed micromixer for a Re = 0.1. In order to use the UCCFM in operation with higher flow rates or with highly viscous fluids, the micromixer design should be optimized, as for example, using of alternate circular obstacles to reduce more the flow cross section, increasing the velocity and then inducing an effective split and recombination mechanism.

4. Conclusion

Cross flow micromixers with circular obstacles were proposed. Water-ethanol and oil-ethanol mixing performance were evaluated ranging the Reynolds number from 0.01 to 100. For both systems, the highest performance indexes were noticed at Re = 0.01, flow regime where molecular diffusion controls the mass transfer between the species. The UCCFM design with d = 600 μm allowed a good fluid mixing for water-ethanol at Re = 0.01 (MI = 0.815) with a very low pressure drop of 0.123 Pa. For oil-ethanol mixing, the MI = 0.693 was obtained for a pressure drop of 76.06 Pa. The application of UCCFM in higher flow rates or with viscous mixtures requires further optimization, as for example, using of alternate circular obstacles or other static obstacles inducing effective advection and split and recombination mechanism.

Acknowledgments

The authors acknowledge the financial support provided by CNPq (National Council for Scientific and Technological Development, Process 404760/2016-3), FAPEMIG (Minas Gerais Research Foundation, Process APQ-02144-17) and FAPESP (São Paulo Research Foundation, Process 2016/20842-4).

References

Castell O.K., Allender C.J., Barrow D.A., 2009, Liquid–liquid phase separation: characterisation of a novel device capable of separating particle carrying multiphase flows. Lab on a Chip, 9, 388-396.

Celik I.B., Ghia U., Roache P.J., Freitas C.J., Coleman H., Raad P.E., 2008. Procedure for Estimation and Reporting of Uncertainty Due to Discretization in CFD Applications. Journal of Fluids Engineering, 130, 078001-1-4.

Cerbelli, S., Borgogna, A., Murmura, M.A., Annesini, M.C., Palocci, C., Bramosanti, M., Chronopoulou, L., 2017, A Tunable Microfluidic Device to Investigate the Influence of Fluid-Dynamics on Polymer Nanoprecipitation, Chemical Engineering Transactions, 57, 853-858

Pistoresi C., Fan Y., Luo L., 2015, Numerical study on the improvement of flow distribution uniformity among parallel mini-channels. Chemincal Engineering and Processing, 95, 63-71.

Pohar A., Plazl I., 2009, Process Intensification through Microreactor Application, Chemical and Biochemical Engineering Quarterly, 23, 537-544.

Santana H.S., Amaral R.L., Taranto O.P., 2015, Numerical study of mixing and reaction for biodiesel production in spiral microchannel. Chemical Engineering Transactions, 43, 1663-1668.

Santana H.S., Tortola D.S., Silva Jr. J.L., Taranto O.P., 2017, Biodiesel synthesis in micromixer with static elements. Energy Conversion and Management, 141, 28-39.

Santana H.S., Tortola D.S., Reis E.M., Silva Jr. J.L., Taranto O.P., 2016, Transesterification reaction of sunflower oil and ethanol for biodiesel synthesis in microchannel reactor: Experimental and simulation studies. Chemical Engineering Journal, 302, 752-762.

Silva Jr., J.L., Santana, H.S., Sanchez, G.B., Taranto, O.P., 2017, Numerical simulation of excess ethanol evaporation from biodiesel in a micro heat-exchanger. Chemical Engineering Transactions, 57, 1123-1128.

Whitesides G.M. The origins and the future of microfluidics., 2006, Nature, 442, 368-373.

Zhou T., Liu T., Deng Y., Chen L., Qian S., Liu Z., 2017, Design of microfluidic channel networks with specified output flow rates using the CFD‐based optimization method. Microfluidics and Nanofluidics, 21:11.